# Wnt/Wingless Pathway Activation Is Promoted by a Critical Threshold of Axin Maintained by the Tumor Suppressor APC and the ADP-Ribose Polymerase Tankyrase

**Zhenghan Wang,*[,1] Ofelia Tacchelly-Benites,*[,1] Eungi Yang,* Curtis A. Thorne,[†,2] Hisashi Nojima,[‡] Ethan Lee,[†,§] and Yashi Ahmed*[,3]**

*Department of Genetics and the Norris Cotton Cancer Center, Geisel School of Medicine at Dartmouth College, Hanover, New Hampshire 03755, [†]Department of Cell and Developmental Biology and [§]Vanderbilt Ingram Cancer Center and Vanderbilt Institute of Chemical Biology, Vanderbilt University Medical Center, Nashville, Tennessee 37232, and [‡]The Francis Crick Institute, Mill Hill Laboratory, London NW7 1AA, United Kingdom

**ABSTRACT** Wnt/β-catenin signal transduction directs metazoan development and is deregulated in numerous human congenital disorders and cancers. In the absence of Wnt stimulation, a multiprotein "destruction complex," assembled by the scaffold protein Axin, targets the key transcriptional activator β-catenin for proteolysis. Axin is maintained at very low levels that limit destruction complex activity, a property that is currently being exploited in the development of novel therapeutics for Wnt-driven cancers. Here, we use an *in vivo* approach in *Drosophila* to determine how tightly basal Axin levels must be controlled for Wnt/Wingless pathway activation, and how Axin stability is regulated. We find that for nearly all Wingless-driven developmental processes, a three- to fourfold increase in Axin is insufficient to inhibit signaling, setting a lower-limit for the threshold level of Axin in the majority of *in vivo* contexts. Further, we find that both the tumor suppressor adenomatous polyposis coli (APC) and the ADP-ribose polymerase Tankyrase (Tnks) have evolutionarily conserved roles in maintaining basal Axin levels below this *in vivo* threshold, and we define separable domains in Axin that are important for APC- or Tnks-dependent destabilization. Together, these findings reveal that both APC and Tnks maintain basal Axin levels below a critical *in vivo* threshold to promote robust pathway activation following Wnt stimulation.

**KEYWORDS** APC; Axin; Tankyrase; Wingless

THE Wnt/Wingless signal transduction pathway directs fundamental processes in metazoans, whereas Wnt pathway deregulation underlies numerous human congenital disorders and cancers (MacDonald *et al.* 2009; Clevers and Nusse 2012). The development of >80% of colorectal cancers is triggered by inactivation of the tumor suppressor adenomatous polyposis coli (APC), which results in the aberrant activation of Wnt signaling. APC is part of a "destruction complex" that includes the scaffold protein Axin, and two kinases: glycogen synthase kinase 3 and casein kinase 1α. Under basal conditions, the destruction complex targets the key transcriptional activator β-catenin for proteasomal degradation. Following Wnt stimulation, destruction complex activity is inhibited, resulting in increased concentrations of cytoplasmic and nuclear β-catenin and the transcriptional regulation of Wnt target genes (MacDonald *et al.* 2009; Clevers and Nusse 2012).

Biochemical studies in *Xenopus* egg extracts revealed that the concentration of Axin is several magnitudes lower than that of other destruction complex components (Salic *et al.* 2000; Lee *et al.* 2003). Because Axin is an essential scaffold for destruction complex assembly, its limiting concentration was proposed to dictate the amount of β-catenin that is


doi: 10.1534/genetics.115.183244
Manuscript received November 19, 2015; accepted for publication January 18, 2016; published Early Online March 10, 2016.
Supplemental material is available online at www.genetics.org/lookup/suppl/doi:10.1534/genetics.115.183244/-/DC1.
[1]These authors contributed equally to this work.
[2]Present address: Department of Pharmacology, Green Center for Systems Biology, Simmons Cancer Center, University of Texas Southwestern Medical Center, Dallas, TX 75390.
[3]Corresponding author: Department of Genetics and the Norris Cotton Cancer Center, Geisel School of Medicine at Dartmouth College, HB 7400, Hanover, NH 03755. E-mail: yfa@dartmouth.edu

targeted for degradation. Supporting this model, Axin overexpression inhibits Wnt signaling (Zeng *et al.* 1997; Hamada *et al.* 1999; Willert *et al.* 1999), whereas Axin inactivation results in the constitutive activation of the Wnt pathway *in vivo* (Hamada *et al.* 1999; Willert *et al.* 1999).

The mechanisms controlling Axin stability are not fully understood, but previous studies have implicated roles for APC (Takacs *et al.* 2008), Protein Phosphatase 1 (Luo *et al.* 2007) and the Wnt coreceptor LRP6 (Tolwinski *et al.* 2003; Cselenyi *et al.* 2008) in regulating Axin proteolysis. More recently, the ADP-ribose polymerase Tankyrase (Tnks) was found to target Axin for proteasomal degradation (Huang *et al.* 2009). Small molecule inhibitors of Tnks disrupt Wnt signaling in cultured colon carcinoma cells by stabilizing Axin (Chen *et al.* 2009; Huang *et al.* 2009) and impede the growth of Wnt pathway-dependent intestinal adenomas in mice (Waaler *et al.* 2012; Lau *et al.* 2013). These findings have suggested a promising new therapeutic strategy based on agents that increase Axin concentration to target Wnt-driven cancers.

Here, we investigate how tightly Axin levels must be controlled to permit the activation of signaling following Wingless stimulation, and we examine the factors that regulate Axin stability. We find that for nearly all Wingless-driven developmental processes, a three- to fourfold increase in Axin was insufficient to inhibit signaling, setting a lower limit for the threshold level of Axin in the majority of *in vivo* contexts. Further, inactivation of Tnks increases Axin levels by twofold, which remain below the threshold at which signaling is inhibited in nearly all *in vivo* contexts. We find, however, that increases in *Axin* transcription that do not disrupt Wingless signaling in wild-type flies are sufficient to inhibit Wingless-dependent developmental processes in *Tnks* mutants. These results highlight the critical function of Tnks in buffering Axin activity. Moreover, we demonstrate that like Tnks, APC also has an evolutionarily conserved role in promoting Axin destabilization, and that separable proteolysis pathways requiring APC or Tnks function through distinct Axin domains to promote Axin degradation. Together, these findings define the *in vivo* threshold for Axin and reveal the important roles of APC and Tnks in maintaining Axin below this critical threshold to promote robust Wnt/Wingless pathway activation.

## Materials and Methods

### *Fly stocks and transgenes*

The *BAC Axin-V5* was constructed using an *Axin* BAC clone (CH321-39B08) containing 110 kb surrounding the *Axin* locus (Gerlach *et al.* 2014). A V5 tag was inserted at the carboxy terminus of the Axin coding region using recombineering as described previously (Venken *et al.* 2009) and verified by sequencing. The modified BAC was introduced using ϕC31-mediated integration at the VK30 (PBac{y[+]-attP-9A}VK00030) or VK33 (PBac{y[+]-attP-3B}VK00033) docking sites.

To generate the *pUASTattB-AxinΔTBD-V5* transgene, residues D-12 through K-32 were deleted by PCR-based mutagenesis of *pUASTattB-Axin-V5* (Yang *et al.* 2016) using the oligonucleotide: 5′-GGT ATC TGC TAC CCC TTC GGT CAT ATG TTT CCG GAT TCC-3′. The resulting *AxinΔTBD-V5* fragment was digested with *Kpn*I and *Xba*I and then inserted into the *pUASTattB* vector at the *Kpn*I and *Xba*I sites. To generate the *pUASTattB-AxinΔRGS-V5* transgene, residues T-54 through Y-168 were deleted by PCR-based mutagenesis of *pUASTattB-Axin-V5*. The resulting *AxinΔRGS-V5* fragment was digested with *Kpn*I and *Xba*I and then inserted into the *pUASTattB* vector at the *Kpn*I and *Xba*I sites. Transgenic flies were generated using site-specific integration at the *attP33* site using ϕC31-based integration (Bischof *et al.* 2007).

A complete deletion of the *Axin* gene, $Axin^{18}$, was isolated by FLP-mediated *trans*-recombination between FRT sites (Parks *et al.* 2004) in $PBac\{RB\}Mgat2^{e01270}$ and $PBac\{WH\}Axn^{f01654}$ (Exelixis Collection, Harvard Medical School). Potential deletions were identified by lethal complementation tests with the mutant allele $Axin^{s044230}$.

Other stocks are as follows: $Tnks^{19}$ (Wang *et al.* 2016), $Tnks^{503}$ (Wang *et al.* 2016), *C765-Gal4* (Bloomington *Drosophila* Stock Center, BDSC) (Brand and Perrimon 1993), *71B-Gal4* (BDSC) (Brand and Perrimon 1993), $Axin^{s044230}$ (Hamada *et al.* 1999), $Apc2^{33}$ (Takacs *et al.* 2008), $Apc2^{19.3}$ (Takacs *et al.* 2008), $Apc1^{Q8}$ (Ahmed *et al.* 1998), *hsFLP1* (Golic and Lindquist 1989), *FRT82B arm-lacZ* (Vincent *et al.* 1994) (provided by J. Treisman, Skirball Institute, New York), *hsFLP1* (Golic and Lindquist 1989), *vestigial-Gal4 UAS-FLP* (Chen and Struhl 1999), *FRT82B* $ovo^{D1}$ (Chou and Perrimon 1992), and *UAS-attB-Axin-V5* (Yang *et al.* 2016). Canton-S flies were used as wild-type controls. All crosses were performed at 25° unless otherwise indicated.

### *Generation of somatic mitotic clones*

Somatic mitotic mutant clones were generated by *FLP*-mediated recombination (Xu and Rubin 1993) using *hsFLP1* or *vestigial-Gal4 UAS-FLP*. When using *hsFLP1*, clones were induced by subjecting first and second instar larvae to a 37° heat shock for 2 hr and were detected by the loss of expression of an *arm-lacZ* transgene in third instar larval wing imaginal discs.

### *Genotypes for generating mitotic clones*

The genotypes for generating mitotic clones were as follows:

*Tnks* mutant clones expressing *Axin-V5* with the *71B* driver: *hsFLP1/+; UAS-Axin-V5/+; FRT82B* $Tnks^{19}$*/71B-Gal4 FRT82B arm-lacZ*.

*Tnks* mutant clones expressing *Axin-V5* with the *C765* driver: *hsFLP1/+; UAS-Axin-V5/+; FRT82B* $Tnks^{19}$*/C765-Gal4 FRT82B arm-lacZ*.

*Apc1 Apc2* double mutant clones expressing *Axin-V5* with the *vestigial* driver: *vestigial-Gal4 UAS-FLP /+; UAS-Axin-V5/+; FRT82B* $Apc2^{33}Apc1^{Q8}$*/FRT82B arm-lacZ*.

*Apc1 Apc2* double mutant clones mutant clones expressing *Axin-V5* with the *C765* driver: *hsFLP1/+; UAS-Axin-V5/+; FRT82B* $Apc2^{33}Apc1^{Q8}$*/C765-Gal4 FRT82B arm-lacZ*.

### Generation of germline clones

*Apc1 Apc2* double null mutant germline clones were generated using the *FLP-DFS* technique (Chou and Perrimon 1992). First and second instar larvae of the genotype *hsFLP1/+; FRT82B ovo$^{D1}$/FRT82B Apc2$^{19.3}$ Apc1$^{Q8}$* were heat shocked for 2 hr and subsequently as adults were crossed to *Apc2$^{19.3}$ Apc1$^{Q8}$/TM6B* males. Lysates for immunoblots were made from their embryos at 0–2 hr of development.

### Antibodies

The primary antibodies used were guinea pig anti-Axin (1:1000) (Wang *et al.* 2016), mouse anti-V5 (1:5000 for immunoblots; Invitrogen), rabbit anti-V5 (1:2000 for immunostaining; Abcam), mouse anti-Wingless (1:20, 4D4; Developmental Studies Hybridoma Bank, DSHB); mouse anti-Engrailed (1:100, 4D9; DSHB), guinea pig anti-Senseless (1:1000) (Nolo *et al.* 2000), guinea pig anti-Apc2 (1:5000) (Ahmed *et al.* 2002; Takacs *et al.* 2008), rabbit anti-β-gal (1:1000; MP Biomedicals), mouse anti-β-gal (1:1000; Promega), rabbit anti-GFP (1:200; Invitrogen), mouse anti-α-tubulin (1:4000; Sigma), and rabbit anti-Kinesin Heavy Chain (1:10,000; Cytoskeleton).

Secondary antibodies used for immunostaining were goat or donkey Alexa Fluor 488, 555, or 568 conjugates (1:400; Invitrogen), and goat Cy5 conjugates (1:200; Jackson ImmunoResearch). Secondary antibodies used in immunoblots were guinea pig and rat peroxidase conjugates (1:5000; Jackson ImmunoResearch) or mouse and rabbit peroxidase conjugates (1:10,000; Biorad).

### Immunostaining, immunoblotting, and quantification

For immunostaining, third instar larval wing imaginal discs were dissected in PBS, fixed in 4% paraformaldehyde in PBS for 20 min, and washed with PBS with 0.1% Triton X-100, followed by incubation in PBS with 0.5% Triton X-100 and 10% BSA for 1 hr at room temperature. Incubation with primary antibodies was performed at 4° overnight in PBS with 0.5% Triton X-100. Incubation with secondary antibodies was for 2 hr at room temperature. Fluorescent images were obtained on a Nikon A1RSi confocal microscope and processed using Adobe Photoshop software. Quantification of immnuostaining was performed with NIS Elements (Nikon). The same region of interest (ROI, with area of 5–10 $\mu m^2$) was placed in the adjacent cells with different genotypes (wild-type and *71B > Axin-V5* for Figure 2C; *Axin-V5* and *Axin-V5*; *Tnks* for Figure 2O). Mean intensity was obtained for each ROI and the relative intensity was calculated for the two correlated ROIs. A total of 20–30 measurements were done for each experiment.

For immunostaining of embryos, embryos were dechorionated and then fixed in 3.7% formaldehyde and rehydrated in PBT (PBS with 0.1% Tween-20, and 1% BSA). Following incubation for 1 hr in blocking solution (PBS with 0.1% Tween-20 and 10% BSA), embryos were incubated overnight at 4° with primary antibodies in PBT. After washing with PTW (PBS with 0.1% Tween-20), embryos were incubated with secondary antibodies for 1 hr at room temperature. Embryos were then washed with PTW and mounted in Prolong Gold (Invitrogen).

For larval lysates used in immunoblots, third instar larvae were dissected to remove salivary glands, fat body, and gut tissues in cold PBS. After removal of PBS, 4× Laemmli loading buffer was added and the lysates were vortexed briefly and incubated for 5 min at 100° before SDS-PAGE analysis. Embryos were homogenized in 4× Laemmli loading buffer, and lysates were incubated at 100° for 5 min. Quantification of immunoblots was performed with ImageJ (Wayne Rasband, National Institutes of Health).

### Immunoprecipitation

For immunoprecipitation experiments, S2R+ cells were harvested 48 hr after transfection, washed with 1× PBS, then lysed in lysis buffer [50 mM Tris-HCl (pH 8.0), 100 mM NaCl, 1% NP-40, 10% glycerol, 1.5 mM EDTA (pH 8.0)] supplemented with 1 μM ADP-HPD (Enzo Life Sciences) and phosphatase and protease inhibitor cocktail (1:100, Thermo Scientific). Lysates were incubated with mouse anti-V5 antibody (Invitrogen) overnight at 4°, followed by addition of protein A/G-sepharose beads (Santa Cruz) for 1 hr at 4°. Beads were washed three times with wash buffer [50 mM Tris-HCl (pH 8.0), 150 mM NaCl, 1% NP-40, 10% glycerol, 1.5 mM EDTA (pH 8.0)] supplemented with 1 μM ADP-HPD and phosphatase and protease inhibitor cocktail (1:100), and boiled with 4× sample buffer supplemented with 0.1 M DTT. Samples were resolved by SDS-PAGE and immunoblotted with the indicated antibodies.

### Cell culture and transfection

S2R+ cells (*Drosophila* Genomics Resource Center) were maintained at 25° in Schneider's complete medium: Schneider's *Drosophila* medium with L-glutamine (Gibco) supplemented with 10% FBS (Gibco) and 0.1 mg/ml penicillin/streptomycin (Invitrogen). Cells were transiently transfected using calcium-phosphate DNA precipitation (Graham and van der Eb 1973).

### Plasmids

Plasmids used for transfection of *Drosophila* cells were *pAc5.1-Axin-V5*, *pAc5.1-AxinΔTBD-V5*, and *pAc5.1-AxinΔRGS-V5*. To generate the plasmids *pAc5.1-Axin-V5*, *pAc5.1-AxinΔTBD-V5*, and *pAc5.1-AxinΔRGS-V5*, fragments encoding *Axin-V5*, *AxinΔTBD-V5*, and *AxinΔRGS-V5* from *pUASTattB-Axin-V5*, *pUASTattB-AxinΔTBD-V5*, and *pUASTattB-AxinΔRGS-V5*, respectively, were digested using *Kpn*I and *Xba*I. The resulting fragments were inserted into the *pAc5.1 A* vector (Invitrogen) at the *Kpn*I and *Xba*I sites.

### Double-stranded RNA generation and RNAi-mediated knockdown

Generation of double-stranded RNAs (dsRNAs) and dsRNA-mediated knockdown were performed as described previously

(Rogers and Rogers 2008). Briefly, DNA templates of 200–900 nucleotides in length targeting *Axin* or the *white* negative control (Zhang *et al.* 2011) were generated by PCR from genomic DNA extracted from S2R+ cells. PCR templates contained T7 promoter sequences on both ends. The DNA templates were amplified using the following primer pairs:

*white*: forward 5′-T7-ACCTGTGGACGCCAAGG-3′ and reverse 5′-T7-AAAAGAAGTCGACGGCTTC-3′ and
*Axin*: forward 5′-T7-CACAAAATAAAGAAGCAGCAGACGG-3′ and reverse 5′-T7-ATTTGATTGTAGCTTTAACGGCTGG-3′.

dsRNAs were transcribed from PCR-generated templates using the T7 Megascript kit (Ambion) according to the manufacturer's instructions. For RNAi-mediated knockdown, S2R+ cells were plated in 10-cm$^2$ plates with 2.5 ml of serum-free, antibiotic-free Schneider's medium with L-glutamine. A total of 25 μg of each dsRNA was added to the medium and cells were incubated with gentle rotation at room temperature for 1 hr. Following incubation, 2.5 ml of complete medium was added and cells were incubated at 25°. After 24 hr, the medium was removed from the cells. This procedure was repeated once every 24 hr for a total of 96 hr.

### *Xenopus assays*

Preparation of *Xenopus* egg extract and degradation assays, as well as immunodepletion and reconstitution of APC in *Xenopus* egg extracts were performed as previously described (Salic *et al.* 2000). For Axin degradation, egg extracts were supplemented with lithium chloride (25 mM) to enhance turnover. APC antibodies were raised against recombinant MBP-APCm3 (amino acids 1342–2075 of *Xenopus* APC) expressed and purified using the baculovirus/Sf9 system, and the amount of APC added back to *Xenopus* egg extracts was quantified by immunoblotting and compared to a standard curve of MBP-APCm3. MT-Axin and MT-AxinΔRGS were a gift from Frank Costantini (Columbia University, New York). AxinRGS encoding amino acids 1–216 of mouse Axin was cloned into the CS2+ plasmid. Labeled [$^{35}$S] Axin and β-catenin for degradation assays was synthesized *in vitro* using the TNT system (Promega). Capped mRNAs for *Xenopus* embryo injections were synthesized from linearized plasmid DNA templates using mMessage mMachine (Ambion).

### *Data availability*

The authors state that all data necessary for confirming the conclusions presented in the article are represented fully within the article.

## Results

### *An in vivo threshold for Axin in Wingless signaling*

To define the upper threshold for Axin levels that is compatible with Wingless pathway activation in physiological contexts, we sought to increase Axin levels *in vivo* to different extents. However, the quantification of Axin levels has been challenging, as endogenous *Drosophila* Axin had not been detectable by immunoblotting in previous studies, which was thought to result from the very low Axin levels (Willert *et al.* 1999; Tolwinski *et al.* 2003). Thus, detection of endogenous Axin had been dependent on a combination of immunoprecipitation followed by immunoblotting, which made accurate quantification difficult (Willert *et al.* 1999; Tolwinski *et al.* 2003; Peterson-Nedry *et al.* 2008). Recently, we overcame this obstacle by generating a new polyclonal Axin antibody with greatly improved sensitivity that permitted the detection of endogenous Axin (Wang *et al.* 2016). The specificity of this Axin antibody was demonstrated by loss of Axin signal in lysates from cultured embryonic S2R+ cells subjected to RNAi-mediated *Axin* knockdown (Figure 1A).

Having established conditions that permitted detection of endogenous Axin, we examined the effect of increasing Axin levels on Wingless-dependent developmental processes. To increase Axin ubiquitously *in vivo*, we generated transgenic flies with a BAC clone that contained 110 kilobases surrounding the *Axin* locus, such that *Axin* was expressed under the control of its endogenous promoter/enhancers (Gerlach *et al.* 2014). A V5 epitope tag was inserted at the carboxy terminus of the *Axin* coding sequence (Venken *et al.* 2009). *BAC Axin-V5* was integrated at a single genomic site on either the second or the third chromosome using site-specific recombination (Markstein *et al.* 2008). Whereas *Axin* inactivation is known to result in fully penetrant embryonic lethality resulting from the aberrant activation of the Wingless pathway (Hamada *et al.* 1999), expression of *BAC Axin-V5* rescued *Axin* null mutants to viability. The rescued adults appeared morphologically wild-type, indicating complete recovery of the many Wingless-dependent developmental processes required for normal development, and importantly, no Wingless loss-of-function phenotypes were observed. These findings indicated that the BAC Axin-V5 protein was fully functional and also expressed at levels subject to physiological regulation.

We next examined how increases in Axin to different levels affected Wingless-dependent processes *in vivo*. In otherwise wild-type flies that were homozygous for the *BAC Axin-V5* transgene on the second or the third chromosome, the Axin protein levels were increased by approximately twofold, as revealed by immunoblotting of larval extracts (Figure 1, B and C). Further, in flies homozygous for the *BAC Axin-V5* transgene on both the second and the third chromosomes, the Axin protein levels were increased by three- to fourfold (Figure 1, B and C). Despite the increased Axin levels, no defects in Wingless-dependent epidermal cell fate specification were observed in embryos, as revealed by the expression of Wingless, the Wingless pathway target gene *engrailed* (Bejsovec and Martinez Arias 1991) (Figure 1, D–I), and by the embryonic hatch rate (Figure 1J). Further, nearly all external structures in adults were morphologically indistinguishable from wild type, indicating that Wingless-dependent developmental processes had not been disrupted. The only process for which we observed a defect was in the

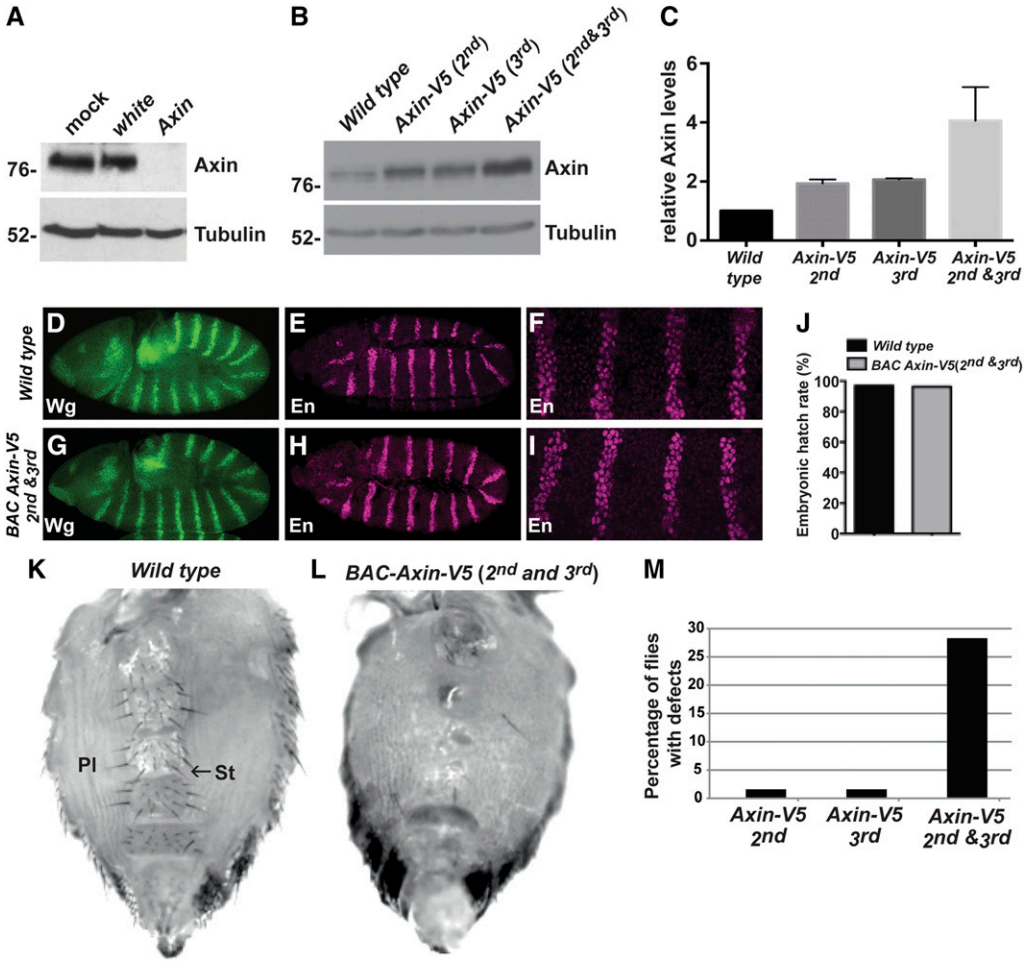


**Figure 1** Threshold above which Axin disrupts Wingless signaling. (A) Lysates from S2R+ cells treated with mock, *white* (negative control), or *Axin* dsRNAs were subjected to immunoblot with Axin antibody. Axin antibody specifically detected endogenous Axin in lysates treated with mock or *white* dsRNA. Tubulin was used as a loading control. (B) Lysates from third instar larvae of the indicated genotypes were subjected to immunoblot with Axin antibody. (C) Quantification of Axin protein levels by immunoblot. Results represent three independent experiments. Values indicate mean ± SD. (D–I) stage 9 or 10 wild-type embryos (D–F), and embryos expressing *BAC Axin-V5* on both the second and third chromosomes (G–I) stained with antibodies against Wingless (Wg) and Engrailed (En). Images in (F) and (I) are higher magnification views of embryos in (E) and (H), respectively. Wg and En expression patterns appeared indistinguishable in wild-type embryos and embryos expressing *BAC Axin-V5*. (J) The hatch rate of wild-type embryos and embryos expressing *BAC Axin-V5*. A total of 100 wild-type embryos and 80 *BAC Axin-V5* embryos were analyzed. (K) Ventral abdomen of wild-type females exhibited normal organization of pleura (Pl), sternites, and sternal bristles (St, arrow). (L) Loss of sternal bristles and expansion of the pleura in flies expressing *BAC Axin-V5* on both the second and third chromosomes. This phenotype was present with varying severity; shown is a representative example. (M) Percentage of flies exhibiting loss of sternal abdominal bristles.

patterning of the adult ventral abdomen. During pupation, Wingless signaling specifies the fate of cells that generate sternites, the bristle-bearing cuticular plates in the ventral abdomen, as well as specifying the cells that generate sensory bristles emanating from the sternites (Baker 1988). A total of 2% of the flies carrying *BAC Axin-V5* on the second or third chromosome, and 28% of the flies carrying *BAC Axin-V5* on both the second and third chromosome displayed loss of one or more sternal bristles, which is indicative of Wingless pathway inhibition (Figure 1, K–M). Together, these findings revealed that increases of three- to fourfold above the endogenous Axin level reach the threshold at which signaling is disrupted in one developmental context; however, the Axin threshold is higher than this for most Wingless-dependent processes during development, consistent with previous work (Peterson-Nedry *et al.* 2008).

### *Tankyrase promotes Wingless signaling by buffering Axin activity*

Axin stability is regulated in part by an ADP-ribose polymerase, Tankyrase (Tnks), which targets Axin for proteasomal degradation (Huang *et al.* 2009). We sought to determine the extent to which the control of basal Axin levels is dependent on Tnks *in vivo*. We isolated two *Tnks* null alleles (Wang *et al.* 2016) and confirmed that Axin protein levels were increased in lysates from *Tnks* mutants by immunoblotting with our Axin antibody (Figure 2A). Quantification of immunoblots revealed a two- to threefold increase in Axin levels in *Tnks* mutants, which is below the physiological threshold at which Axin levels inhibit Wingless pathway activation. This conclusion may explain the observations from recent work, which revealed that *Tnks* inactivation had no effect on Wingless-dependent developmental processes unless Axin was concomitantly overexpressed at levels high enough to inhibit Wingless signaling (Feng *et al.* 2014). In that background, Tnks loss further exacerbated the phenotypes that resulted from Axin overexpression.

However, we reasoned that overexpression of Axin in this prior study, at levels that were high enough to abrogate Wingless signaling, would likely have masked its physiological regulation; thus, we sought to examine the *in vivo* role of Tnks in regulating Axin at levels that remained within

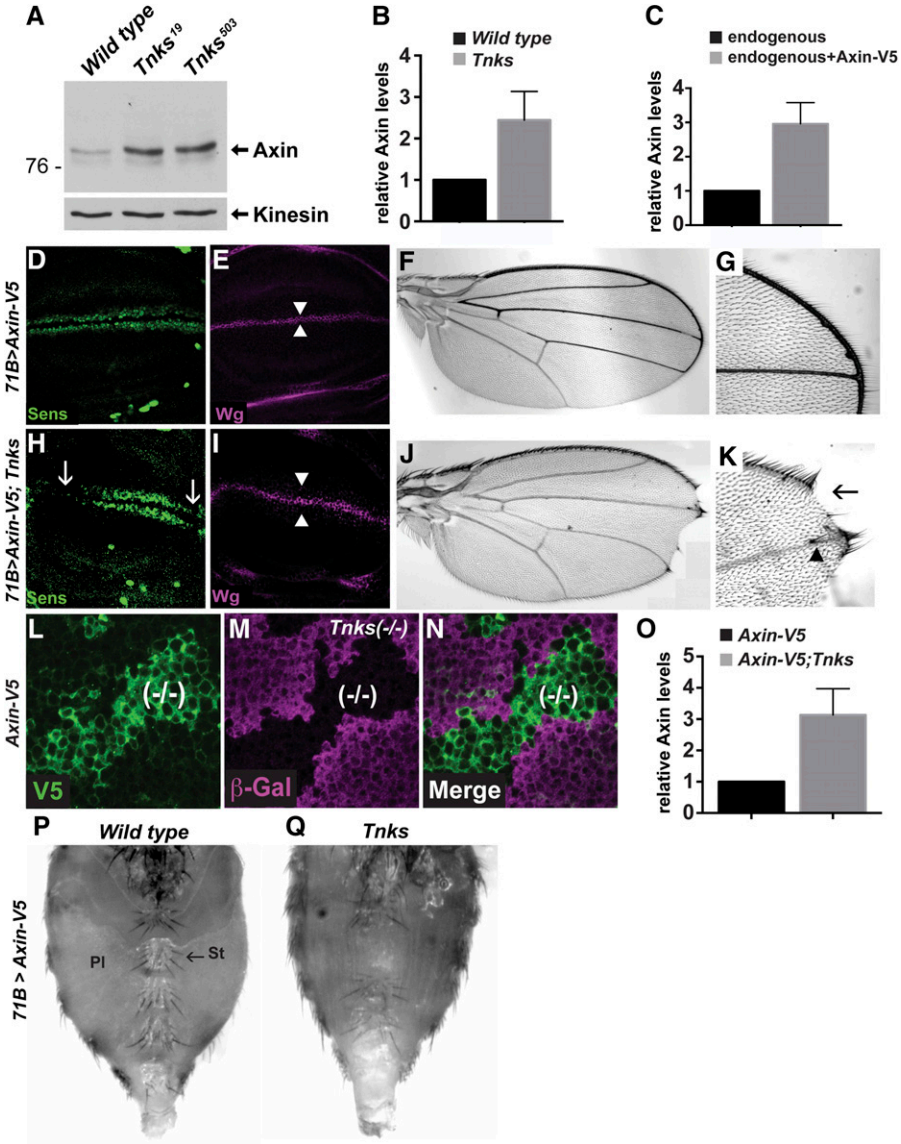


**Figure 2** Tnks promotes Wingless signaling by promoting Axin degradation. (A) Lysates from third instar larvae of the indicated genotypes were subjected to immunoblot with Axin antibody. Kinesin was used as a loading control. (B) Quantification of Axin protein levels by immunoblots with wild-type or *Tnks*$^{19}$ mutant larvae. Result represents four independent experiments. Values indicate mean ± SD. (C) Quantification of Axin levels by immunostaining. Wing discs expressing *Axin-V5* were stained with anti-V5 and anti-Axin antibodies. Axin protein levels were measured by the intensity of Axin antibody staining. Cells that did not express *Axin-V5* were identified by the absence of V5 staining. Values indicate mean ± SD ($n$ = 30). (D and E) Confocal images of third instar larval wing discs expressing *Axin-V5* with the *71B-Gal4* driver. Expression of *Axin-V5* does not disrupt the Wingless target gene *senseless* (D), Wingless expression (E), or cell fate in the adult wing (F and G; 100% of flies had wild-type appearing wings, $n$ = 20). (H and I) Expression of *Axin-V5* with the *71B-Gal4* driver in *Tnks* null mutants (*Tnks*$^{19}$/*Tnks*$^{503}$) results in attenuation of Senseless expression (H, arrows) and a slight increase in the number of cells expressing Wingless (I, arrowheads). In the adult wing, expression of *Axin-V5* in *Tnks* null mutants causes loss of wing blade tissue (J), loss of sensory bristles at the margin (K, arrow), and extra bristles in the wing blade (K, arrowhead; 100% of *Tnks* mutant flies displayed wing margin defects, $n$ = 35). (L–N) Wing disc expressing *Axin-V5* labeled with α-V5 (green), α-β-gal (magenta), and merge. Absence of β-gal staining marks *Tnks*$^{19}$ mutant clones. The levels of Axin-V5 inside *Tnks*$^{19}$ mutant clones are increased compared to that of the surrounding wild-type tissue. Patchy expression from the *71B* driver likely accounts for the few cells within *Tnks* mutant clones in which the Axin-V5 level is not increased. (O) Quantification of Axin protein levels by immunostaining with V5 antibody. *Tnks* mutant clones were induced in wing discs expressing the *Axin-V5* transgene. Intensity of V5 staining was measured inside and outside *Tnks* mutant clones. Values indicate mean ± SD ($n$ = 18). (P) Ventral abdomen of wild-type adult female expressing *Axin-V5* with the *71B-Gal4* driver. Pleura (Pl), sternites (St), and sternal bristles (arrow) display normal organization. Some sternites and sternal bristles are lost in *Tnks*$^{19}$/*Tnks*$^{503}$ mutants (Q), indicating that Tnks promotes Wingless-dependent cell fate specification.

physiological range. We examined Axin regulation in the larval wing imaginal disc, where Wingless signaling is critical for growth and patterning and where inhibition of the Wingless pathway results in well-characterized defects in cell fate specification (Couso *et al.* 1994). We used the UAS/Gal4 system (Brand and Perrimon 1993), which facilitated the conditional expression of Axin tagged with a V5 epitope (Yang *et al.* 2016), or mutant forms of Axin with deletions, for structure–function analysis. To express Axin at near-physiological levels in the wing disc, we screened for Gal4 drivers that permitted Axin expression at levels that did not disrupt Wingless-dependent wing development, and identified two drivers that met these criteria: *71B* and *C765*. To compare the relative level of Axin-V5 driven by *71B-Gal4* with that of endogenous Axin, we took advantage of our Axin antibody, which permits sensitive detection of endogenous Axin by immunostaining of imaginal discs (Supplemental Material, Figure S1). Wing discs expressing the *Axin-V5* transgene were stained with both anti-V5 and anti-Axin antibodies. Quantification of the Axin and V5 signals revealed a threefold increase in Axin levels in wing disc cells expressing Axin-V5, by comparison with neighboring wild-type cells that did not express Axin-V5 (Figure 2C). As expected, under these conditions, both the expression of the Wingless target gene *senseless* at the dorsoventral boundary of the third instar larval wing imaginal disc, and the morphology of the adult wing margin were indistinguishable from wild-type (Figure 2, D–G). These findings indicated that under these conditions, Axin was expressed at levels that were subject to physiological regulation.

Having established conditions at which Axin was expressed within physiological range, we sought to determine the effects of Tnks inactivation on Axin activity. We found that expression of *Axin-V5* in *Tnks* null mutants under the same conditions resulted in loss of *senseless* at the dorsoventral boundary of the larval wing imaginal discs, loss of sensory bristles at the adult wing margin, notched wings, and ectopic bristles in the wing blade (Figure 2, H–K); each of these defects is indicative of inhibition of Wingless signaling. Similar results were observed with the *C765-Gal4* driver (see below, Figure 5, D–G), and thus we used these two drivers interchangeably in subsequent studies. These findings reveal that increases in Axin levels that are compatible with normal signaling in wild-type flies markedly inhibited signaling upon Tnks inactivation.

To identify the extent to which Axin levels were increased in *Tnks* mutant wing discs cells, we compared *Axin-V5* levels in wild-type cells that were juxtaposed with *Tnks* null mutant cells. As expected, we found the levels of Axin-V5 were higher in *Tnks* mutant clones compared with the surrounding tissue (Figure 2, L–N), consistent with the known role of Tnks in promoting Axin degradation. Quantification of the Axin immunofluorescence intensity revealed a threefold increase in Axin-V5 levels in *Tnks* null mutant cells (Figure 2O). As expression of Axin-V5 in wild-type cells resulted in a threefold increase above endogenous Axin levels, and elimination of Tnks resulted in an additional threefold increase, we postulated that the threshold at which Axin levels inhibited Wingless signaling in wing discs is between three and ninefold above the endogenous Axin level. These findings provided additional evidence to support the hypothesis that Tnks-dependent Axin proteolysis buffers Axin activity.

To determine whether Tnks has the same function in other physiological contexts, we examined a different developmental stage and tissue. When transgenic *Axin* was expressed in the pupal abdomen with the *71B-Gal4* driver, Wingless-dependent cell fate specification was indistinguishable from wild-type, as revealed by the size, morphology, spacing, and number of sternites and sternal bristles in adults (compare Figure 1K and Figure 2P). These findings indicated that the levels of Axin expressed under these conditions remained within the range that is subject to physiological regulation. In contrast, under the same conditions, the abdomens of *Tnks* null mutant adults displayed a reduced number of sternites and sternal bristles, a decreased size in the sternites that remained, and expansion of the pleura (Figure 2Q). These phenotypes are indicative of loss of Wingless signaling, as observed previously in *wingless* mutants, or upon inactivation of the Wingless pathway transcriptional activators dTCF/Pangolin and Legless/BCL9 (Baker 1988; Brunner *et al.* 1997; Kramps *et al.* 2002). Thus, as observed in the wing, increases in *Axin* transcription that are compatible with normal development in the wild-type abdomen inhibit Wingless-dependent developmental processes following Tnks inactivation. These findings provided evidence that Tnks-dependent Axin proteolysis serves to buffer Axin activity in multiple *in vivo* contexts.

### *APC-dependent Axin proteolysis controls basal Axin levels in vivo*

As we had found that Axin levels increased by only two- to threefold following Tnks loss, we hypothesized that other degradation pathways also function to maintain Axin below the *in vivo* threshold compatible with Wingless signaling. Therefore, we further investigated our previous discovery that the two fly homologs of the APC tumor suppressor facilitate the control of basal Axin levels (Takacs *et al.* 2008). Consistent with our previous results, we found that in larval wing discs expressing *Axin-V5*, the levels of Axin-V5 were higher in *Apc1 Apc2* double mutant clones as compared with surrounding tissues (Figure 3, A–C). Importantly, the increased Axin staining intensity in *Apc* mutant clones was detected throughout the cell, revealing that the increased staining was not secondary to a change in the subcellular localization of Axin. These findings suggested that APC destabilizes Axin.

To further test this conclusion, we utilized our new Axin antibodies, which allowed analysis of the effect of *Apc* inactivation on endogenous Axin levels with immunoblots, and thus provided an independent test of the regulation of Axin by Apc. Axin immunoblots revealed that by comparison with lysates from wild-type larvae, Axin levels were increased in lysates from *Apc2* mutant larvae to an extent similar to that in *Tnks* null mutants (Figure 3D). We also sought to determine the effect of simultaneous elimination of Apc1 and Apc2 on Axin levels; however, since loss of Apc1 and Apc2 results in lethality during larval development (Ahmed *et al.* 2002; Akong *et al.* 2002), we examined Axin levels in lysates from *Apc1 Apc2* double null mutant embryos. By comparison with wild-type embryos, Axin levels were increased in *Apc1 Apc2* double mutants (Figure 3E), consistent with previous findings of increased Axin levels in *Apc1 Apc2* double mutant clones in imaginal discs revealed by immunostaining (Takacs *et al.* 2008). Of note, one-half of these mutant embryos have wild-type Apc supplied paternally; therefore, the level to which Axin is increased following Apc inactivation is likely higher. Nonetheless, the increased Axin levels in *Apc1 Apc2* double mutant and *Tnks* mutant embryos were present by 2 hr of development, which is prior to the onset of Wingless expression. Together, these findings indicate that like Tnks, Apc also negatively regulates the basal levels of Axin, independently of Wingless exposure.

### *APC has an evolutionarily conserved role in regulating Axin stability*

To determine whether the regulation of Axin by APC is an evolutionarily conserved process, we reconstituted cytoplasmic degradation of β-catenin and Axin in a cell-free system using *Xenopus* egg extracts as previously described (Salic *et al.* 2000; Lee *et al.* 2003). To determine if APC regulates Axin turnover in vertebrates, *Xenopus* egg extracts were immunodepleted of APC. APC-immunodepleted extracts resulted in a slower rate of Axin degradation compared to

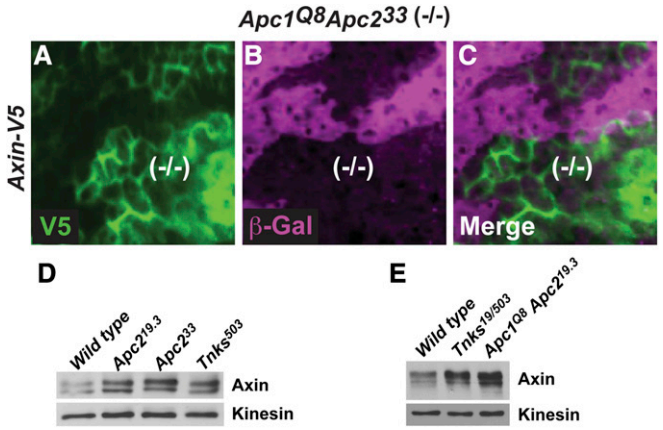


**Figure 3** Apc promotes Axin proteolysis. (A–C) Wing disc expressing *Axin-V5* labeled with α-V5 (green), α-β-gal (magenta), and merge. Absence of β-gal staining marks $Apc1^{Q8}Apc2^{33}$ mutant clones. The levels of Axin-V5 inside $Apc1^{Q8}Apc2^{33}$ mutant clones were increased compared to that of the surrounding wild-type tissue. (D) Larval lysates from indicated genotypes were analyzed by immunoblot using Axin antibody. Axin protein levels were increased in lysates from *Tnks* and *Apc2* mutant larvae. Kinesin was used as a loading control. (E) Lysates from embryos 0–2.5 hr old were analyzed by immunoblot using Axin antibody. Axin protein levels were increased in lysates from *Tnks* and *Apc1 Apc2* double mutant embryos. One-half of the *Apc1 Apc2* double mutant embryos expressed wild-type *Apc1* and *Apc2* from the paternal alleles. Kinesin was used as a loading control.

mock-depleted extracts (Figure 4, A and B). As expected, the rate of β-catenin degradation was also reduced in extracts depleted of APC (Lee *et al.* 2003) (Figure 4B). Addition of immunoprecipitated APC complexes to APC-depleted extracts, however, stimulated the rate of Axin turnover in a dose-dependent manner (Figure 4C). Adding back APC to levels approaching that of the endogenous protein (100 nM) (Salic *et al.* 2000) maximally stimulated Axin degradation.

To examine the *in vivo* role of APC in Axin degradation in vertebrates, we first tested the effects of perturbing the interaction between Axin and APC (Figure 4D). Messenger RNA (mRNA) encoding Myc-tagged Axin (MT-Axin) was injected either alone or together with mRNA encoding AxinRGS (a protein encoding only the APC binding domain of Axin) into two-cell-stage *Xenopus* embryos, and Axin levels were determined by immunoblotting with Myc antibody. Embryos that were coinjected with *AxinRGS* mRNA displayed increased levels of MT-Axin relative to control, suggesting that inhibition of its interaction with APC increases the stability of MT-Axin *in vivo*. We next tested whether negative regulation of endogenous APC by morpholino oligonucleotide (MO) injection would similarly increase steady-state levels of Axin. Embryos were coinjected with *MT-Axin* mRNA and either an APC MO or a control MO. As shown in Figure 4D, injection of the APC MO decreased levels of APC but elevated levels of MT-Axin relative to the control MO. We conclude that in both flies and vertebrates, APC stimulates Axin destabilization and that as found for Tnks, APC has an evolutionarily conserved role in regulating the basal concentration of Axin.

### *The Tankyrase and APC binding domains in Axin are important for control of basal Axin levels*

To analyze the mechanisms by which Tnks and APC regulate Axin levels, we investigated the roles of the conserved Tnks binding domain (TBD) (Huang *et al.* 2009) and APC binding domain (RGS) (Fagotto *et al.* 1999) of Axin. We generated *Axin* transgenes with deletions in these domains (*AxinΔTBD-V5* and *AxinΔRGS-V5*, respectively) (Figure 5A), and examined the effects of these deletions on Axin levels in the Wingless-responsive embryonic cell line S2R +. Probing of cell lysates with V5 antibody revealed that steady-state levels of both AxinΔTBD-V5 and AxinΔRGS-V5 were increased by comparison to Axin-V5 (Figure 5B). To test this conclusion *in vivo*, we generated transgenic flies expressing *AxinΔTBD-V5* or *AxinΔRGS-V5*. To allow for their direct comparison in the absence of transcriptional position effects, the *UAS-AxinΔTBD-V5* or *UAS-AxinΔRGS-V5* transgenes were inserted at the same site in the genome as *UAS-Axin-V5* using site-specific integration (Markstein *et al.* 2008). Each transgene was expressed in third instar wing disc using the *C765-Gal4* driver. We probed larval lysates with V5 antibody and found that the levels of both AxinΔTBD-V5 and AxinΔRGS-V5 were higher than Axin-V5 (Figure 5C). Together, these results indicate that the Tnks and APC binding domains of Axin are important for the negative regulation of Axin levels.

Based on these findings, we sought to determine whether the Tnks and APC binding domains of Axin promote Wingless signaling *in vivo*. As noted above, Wingless signaling is critical for the growth and patterning of larval wing imaginal discs (Couso *et al.* 1994). Expression of *Axin-V5* using the *C765-Gal4* driver resulted in no developmental defects; Wingless-dependent cell fate specification was the same as in wild-type, as revealed by expression of the Wingless target gene *senseless* (Nolo *et al.* 2000), and by the wild-type morphology and size of the adult wing (Figure 5, D–G). In contrast, expression of *AxinΔTBD-V5* under the same conditions resulted in decreased *senseless* expression at the dorsoventral boundary of wing discs, loss of sensory bristles and blade tissue at the margin of adult wings, an increase in the number of cells near the boundary that express Wingless, and ectopic sensory bristles away from the margin; each of these phenotypes is diagnostic for the inhibition of Wingless signaling (Figure 5, H–K). Similarly, expression of *AxinΔRGS-V5* under the same conditions also resulted in diminished *senseless* expression at the dorsoventral boundary, loss of sensory bristles at the margin, and loss of wing blade tissue, although the phenotypes were not as severe as those resulting from expression of *AxinΔTBD-V5* (Figure 5, L–O). Similar results were observed when we performed the same experiments using the Gal4 driver *71B* (data not shown). Taken together, these findings provide *in vivo* evidence that the Tnks binding domain and the APC binding domain

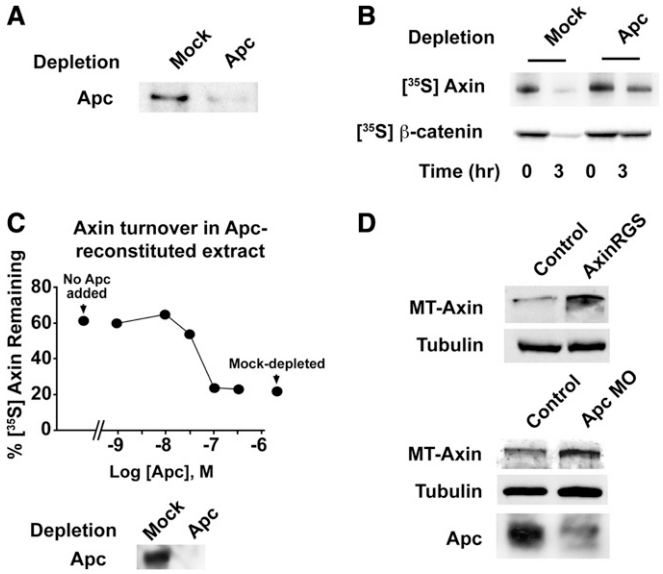


**Figure 4** The destabilization of Axin by APC is conserved in vertebrates. (A) Immunoblotting revealed that the majority of endogenous APC was removed in APC-depleted *Xenopus* egg extracts. (B) Radiolabeled [$^{35}$S] Axin or β-catenin was added to *Xenopus* egg extracts. At the indicated times, samples were withdrawn and subjected to SDS-PAGE/autoradiography. The rate of Axin degradation is reduced in APC-depleted *Xenopus* egg extracts. (C) Apc immunoprecipitated from *Xenopus* egg extracts was titrated into Apc-depleted egg extracts. Radiolabeled Axin was added, samples were removed after 3 hr for SDS-PAGE/autoradiography, and the amount of Axin remaining was quantified. The rate of Axin degradation is regulated by APC in a dose-dependent manner. Concentrations of APC in nondepleted extracts (~100 nM) and amount of APC added back was calculated as described in Lee *et al.* (2003). (D) APC regulates Axin turnover in *Xenopus* embryos. (Top) mRNAs encoding AxinRGS or control (empty vector) plus MT-Axin mRNA (200 pg each) were coinjected into the dorsal blastomeres of four-cell embryos. Embryos were lysed in RIPA buffer at embryonic stage 7 and analyzed by Myc immunoblotting. (Bottom) Control or Apc MO (25 ng) plus mRNA encoding MT-Axin mRNAs (200 pg) was coinjected into the dorsal blastomeres of four-cell-stage embryos. Embryos were then lysed at stage 7 and analyzed by Myc immunoblotting.

facilitate the control of basal Axin levels and the response to Wingless stimulation.

### *Tankyrase and APC promote Axin destabilization through distinct mechanisms*

Next, we sought to compare the mechanisms by which Tnks and APC regulate Axin degradation. As our mutant clonal analysis had revealed that Axin-V5 levels are regulated by both Tnks and Apc *in vivo* (Figure 2, L–N and Figure 3, A–C), this provided a sensitive *in vivo* assay for investigating the regulation of Axin by Apc and Tnks. To determine whether Tnks and APC function in the same Axin proteolysis pathway *in vivo*, we determined whether the domains in Axin required for Tnks- and APC-dependent Axin destabilization were shared. To examine the role of the APC binding domain in Axin (RGS), we expressed *AxinΔRGS-V5* in wing imaginal discs. In contrast with Axin-V5 (Figure 3, A–C), the levels of AxinΔRGS-V5 did not increase in *Apc1 Apc2* double mutant clones; instead, equivalent AxinΔRGS-V5 levels were detected inside and outside the clones (Figure 6, A–C). Thus as expected, deletion of the APC binding domain prevents the ability of APC to negatively regulate Axin. We next tested whether the RGS domain is also important for Tnks-dependent Axin regulation. In contrast with *Apc1 Apc2* double mutant clones, the level of AxinΔRGS-V5 increased markedly in *Tnks* null mutant clones as compared to the surrounding tissue (Figure 6, D–F). These results indicated that Tnks-mediated regulation of Axin does not require Axin's Apc binding domain. We conclude that the destabilization of Axin mediated by Tnks does not require Apc-dependent Axin degradation.

We next examined the importance of the Tnks binding domain (TBD) in Tnks- or APC-mediated Axin destabilization. As expected, deletion of the TBD abolished the ability of Tnks to promote Axin degradation; in contrast with Axin-V5 (Figure 2, L–N), the levels of AxinΔTBD-V5 were indistinguishable inside and outside of *Tnks* null mutant clones (Figure 6, J–L). This finding confirmed that Tnks-mediated Axin degradation requires the TBD. We next examined whether the TBD is also important for APC-dependent Axin degradation. In *Apc1 Apc2* double mutant null clones, the level of AxinΔTBD-V5 was the same as that found in the surrounding tissue (Figure 6, G–I). These findings indicate, unexpectedly, that not only Tnks-mediated degradation, but also Apc-mediated degradation of Axin requires the Tnks binding domain in Axin.

The Axin TBD and RGS domains are juxtaposed (Figure 5A). Thus, deletion of the Axin TBD might result in a conformational change in the Axin RGS domain that indirectly inhibits the interaction between Axin and Apc. To address this possibility, we determined whether deletion of the Axin TBD disrupts the interaction between Axin and Apc. We expressed *Axin-V5*, *AxinΔTBD-V5*, and *AxinΔRGS-V5* in *Drosophila* S2R+ cells. Axin was immunoprecipitated with a V5 antibody and the immunoprecipitates were probed with Apc2 antibody. We detected Apc2 in immunoprecipitates of lysates from cells expressing *Axin-V5* and *AxinΔTBD-V5*. In contrast, we did not detect Apc2 in immunoprecipitates of lysates from cells expressing *AxinΔRGS-V5* (Figure 6M). These results indicate that the Axin TBD is not required for the physical interaction between Axin and APC, and thus that the Axin–APC interaction is important, but not sufficient for APC-mediated Axin degradation. Taken together, these findings indicate that APC and Tnks promote Axin destabilization through partially distinct mechanisms.

## Discussion

Our results demonstrate that regulation of the basal levels of Axin is a dynamic process that requires the activity of the ADP-ribose polymerase Tnks and the tumor suppressor APC. By increasing the gene dosage of *Axin*, we found that endogenous Axin levels can increase by three- to fourfold without reaching the minimal threshold at which Wingless signaling is disrupted in nearly all developing tissues, consistent with

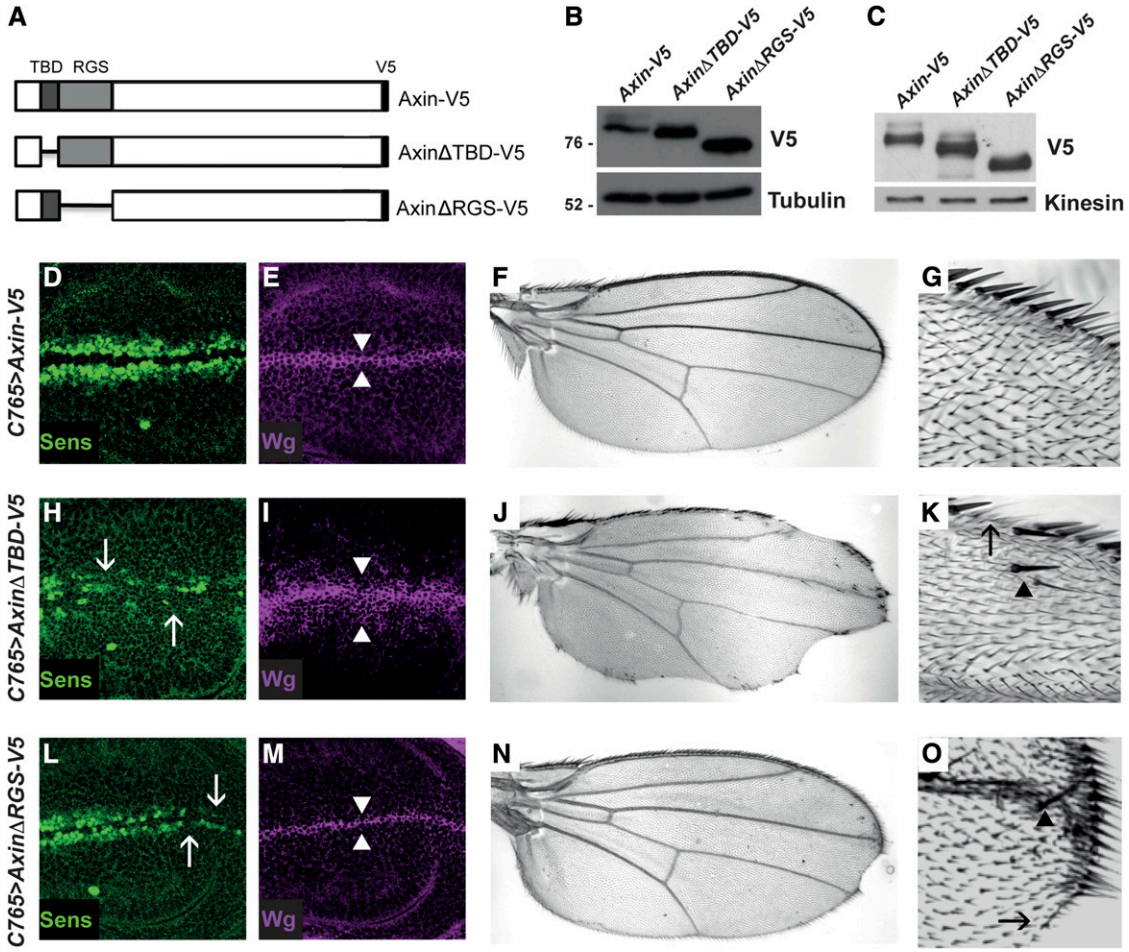


**Figure 5** The Tnks and APC binding domains of Axin are important for promoting Wingless signaling. (A) Schematic representation of *Axin-V5*, *AxinΔTBD-V5*, and *AxinΔRGS-V5*. (B) Lysates of S2R+ cells transfected with the indicated plasmids (250 ng) were analyzed by immunoblotting using a V5 antibody. Deletion of the Tnks binding domain of Axin (*AxinΔTBD-V5*) or the APC binding domain of Axin (*AxinΔRGS-V5*) resulted in aberrant stabilization of Axin compared to wild-type controls (*Axin-V5*). (C) Lysates of third instar larvae expressing the indicated transgenes with *C765-Gal4* driver were analyzed by immunoblotting. AxinΔTBD-V5 and AxinΔRGS-V5 were stabilized compared with Axin-V5 protein. Confocal images of third instar larval wing discs expressing *Axin-V5* (D and E), *AxinΔTBD-V5* (H and I), or *AxinΔRGS-V5* (L and M) with the *C765-Gal4* driver. Staining with Wingless and Senseless antibodies shows that expression of *Axin-V5* did not disrupt expression of the Wingless pathway target Senseless (D) or of the number of cells expressing Wingless (E, arrowheads), indicating that *Axin-V5* was expressed at a level that is compatible with physiological regulation. In contrast, expression of *AxinΔTBD-V5* resulted in loss of Senseless (H, arrows) and expansion in the number of cells expressing Wingless (I, arrowheads), indicating that Wingless signaling is inhibited by *AxinΔTBD-V5*. Expression of *AxinΔRGS-V5* results in loss of Senseless (L, arrows), indicating that *AxinΔRGS-V5* inhibits Wnt signaling. Adult wings expressing *Axin-V5* (F and G), *AxinΔTBD-V5* (J and K), or *AxinΔRGS-V5* (N and O) using the *C765-Gal4* driver are shown. A total of 95% of wings expressing *Axin-V5* (F and G) have normal morphology ($n$ = 136), whereas 92% of wings expressing *AxinΔTBD-V5* (J and K) ($n$ = 127) and 30% of wings expressing *AxinΔRGS-V5* (N and O) ($n$ = 135) display loss of sensory bristles and tissue at the wing margin (K and O, arrow), as well as extra bristles in the wing blade (K and O, arrowhead), which indicate inhibition of Wingless signaling.

previous work (Peterson-Nedry *et al.* 2008). These findings support the hypothesis that Axin levels regulate destruction complex activity, but also reveal that there exists a physiological range of at least three- to fourfold within which Axin levels may fluctuate and yet remain compatible with the activation of the pathway following Wnt stimulation in all cells. This narrow range perhaps serves two essential functions of Axin: (1) degradation of β-catenin to maintain its low levels in the absence of Wnt ligands and (2) robust responsiveness to Wnt stimulation.

These results also provide evidence that Tnks promotes Wingless signaling by maintaining Axin below this *in vivo* threshold. Axin levels increase in the absence of Tnks, but remain below this threshold in nearly all developmental contexts. However, a relatively small increase in *Axin* expression, which in itself has no effect on Wingless-dependent developmental process in wild-type flies, is sufficient to result in classic Wingless loss-of-function phenotypes in *Tnks* mutants. These findings suggest that Tnks-dependent regulation buffers Axin activity and thus is likely important in specific *in vivo* contexts for promoting Wingless signaling.

Our previous work revealed that, whereas complete loss of Apc results in the constitutive activation of Wingless signaling, partial reduction in Apc levels resulted in Wingless

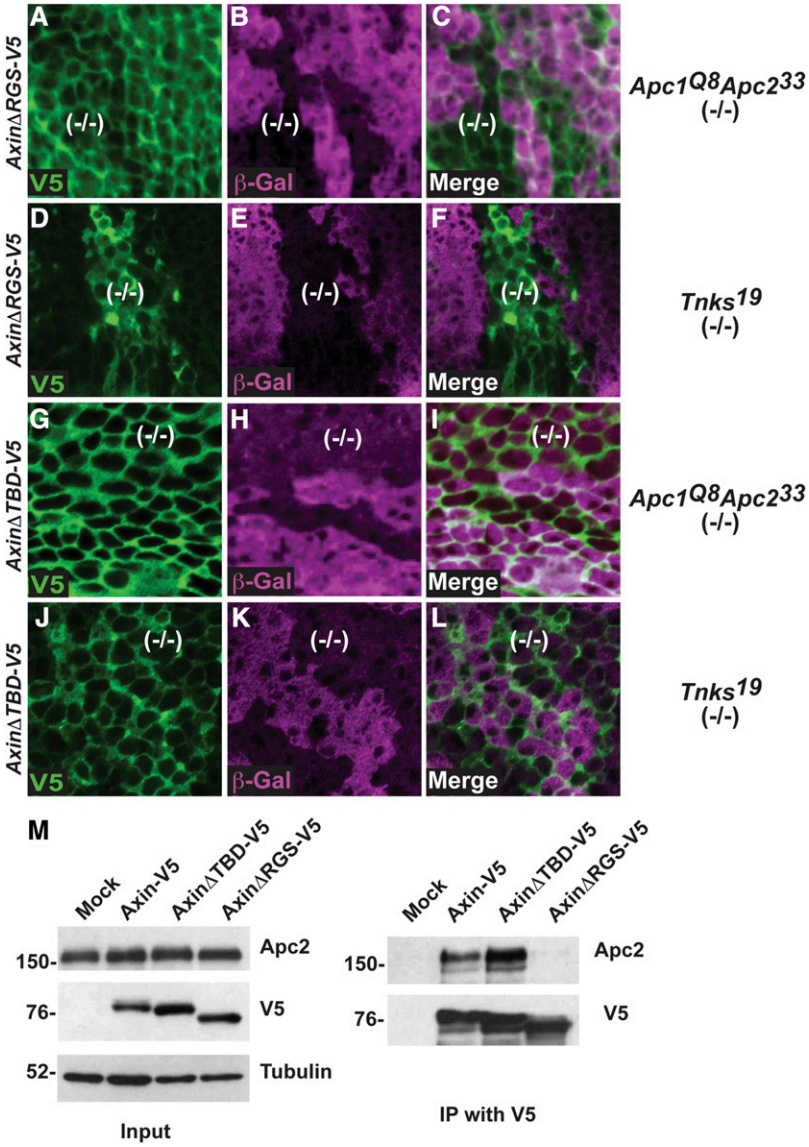


**Figure 6** APC- and Tnks-mediated regulation of Axin are achieved through partially separable mechanisms. Confocal images of third instar larval wing imaginal discs stained with antibodies indicated at bottom left; genotypes are indicated on the right. (A–L) Wing disc labeled with α-V5 (green), α-β-gal (magenta), and merge. Absence of β-gal staining marked *Apc1$^{Q8}$Apc2$^{33}$* mutant clones (A–C and G–I), and *Tnks$^{19}$* mutant clones (D–F and J–L). In contrast with Axin-V5 (Figure 3, A–C), the levels of AxinΔRGS-V5 did not increase inside *Apc1$^{Q8}$Apc2$^{33}$* mutant clones compared to the surrounding wild-type tissue (A–C). The levels of AxinΔRGS-V5 inside *Tnks$^{19}$* mutant clones were increased compared to that of the surrounding wild-type tissue (D–F). In contrast with Axin-V5 (Figure 3, A–C and Figure 2, L–N), the levels of AxinΔTBD-V5 did not increase in *Apc1$^{Q8}$Apc2$^{33}$* mutant clones (G–I) or in *Tnks$^{19}$* mutant clones (J–L) compared to the surrounding wild-type tissue. (M) Immunoprecipitation with V5 antibody from S2R+ cell lysates transfected with *Axin-V5*, *AxinΔTBD-V5*, and *AxinΔRGS-V5*. Apc2 was pulled down with Axin-V5. Deletion of the Tnks binding domain of Axin (AxinΔTBD-V5) had no effect in the interaction between Axin and Apc2. In contrast, deletion of the APC binding domain of Axin (AxinΔRGS-V5) inhibited the interaction with Apc2.

loss-of-function phenotypes in multiple *in vivo* contexts, indicating that Apc has dual negative and positive roles in Wingless signaling (Takacs *et al.* 2008). Our new ability to detect endogenous Axin by immunoblotting provided an independent approach to test the hypothesis that negative regulation of Axin levels contributes to the positive role of Apc in Wingless signaling (Takacs *et al.* 2008). Supporting this hypothesis, Axin levels were aberrantly increased in lysates from *Apc* mutant embryos and larvae. In addition, our studies in frog egg extracts and frog embryos suggest that the function of APC in promoting Axin degradation is evolutionarily conserved. Importantly, the role of APC in Axin degradation, like that of Tnks, is independent of Wingless stimulation. These results suggest that several pathways likely contribute to maintaining basal Axin levels below a critical concentration, above which Wingless signaling is inhibited.

Our findings reveal that Tnks- and Apc-dependent proteolysis of Axin are achieved through partly separable mechanisms. Tnks-mediated Axin destabilization requires the Tnks binding domain of Axin, and thus their physical interaction. Apc-mediated Axin regulation is dispensable for the Tnks-dependent proteolysis of Axin (Figure 6). Conversely, Apc-mediated Axin regulation requires both the Tnks and APC binding domains in Axin (Figure 6). Our analysis reveals that the interaction between Axin and Apc is important, but not sufficient, for APC-mediated Axin degradation (Figure 6). Together, these results suggest that the APC-mediated regulation of Axin involves several distinct domains in Axin and/or a specific Axin conformation.

Given the essential role of Wnt signaling in many fundamental processes, and the requirement that Axin concentrations are maintained below a threshold level for the activation of signaling (Salic *et al.* 2000; Lee *et al.* 2003), it is not surprising that several degradation pathways have evolved to ensure precise control of Axin levels (Luo *et al.* 2007; Cselenyi *et al.* 2008; Takacs *et al.* 2008; Huang *et al.* 2009).

Redundancy in Axin degradation pathways would provide a compensatory fail-safe mechanism to prevent an increase in Axin above its threshold and the resultant inhibition of signaling. Functional redundancy in Axin degradation pathways may also explain why no defects in Wnt-dependent embryonic development were observed upon disruption of fish or fly Tnks (Huang *et al.* 2009; Feng *et al.* 2014; Wang *et al.* 2016). Nonetheless, the high degree of sequence conservation present in Tnks homologs suggests that Tnks loss cannot be fully compensated by other pathways in all *in vivo* contexts. Indeed, small molecule inhibitor studies have indicated that Tnks is important for the Wnt-dependent regeneration of fins following injury in adult fish (Chen *et al.* 2009; Huang *et al* 2009). Moreover, our recent work has revealed that regulation of Axin by *Drosophila* Tnks is required for Wingless target gene activation and the Wingless-dependent control of intestinal stem cell proliferation in the adult midgut (Tian *et al.* 2016; Wang *et al.* 2016). Importantly, in the midgut, Tnks is essential for target gene activation in regions where the Wingless pathway is activated at relatively low levels, but dispensable at high levels (Wang *et al.* 2016), suggesting a critical role for Tnks in the amplification of signaling. Furthermore, we have found that Tnks not only targets Axin for proteolysis, but also promotes the central role of Axin in rapid Wnt pathway activation (Yang *et al.* 2016).

If the basal concentration of human Axin, like that of fly Axin, is determined by several degradation pathways, then small molecule Tnks inhibitors will likely have the greatest therapeutic efficacy in contexts for which Tnks-mediated Axin proteolysis has a predominant role in controlling Axin levels. For example, as APC activity is disrupted in the majority of colorectal carcinomas, APC-dependent Axin degradation is likely compromised in these cells; thus colon carcinoma cells might be particularly sensitive to treatment with Tnks inhibitors, whereas the untransformed neighboring cells that contain wild-type APC levels would be less susceptible. Indeed, in mice for which APC activity has been disrupted by conditional targeting, daily treatment with a small molecule Tnks inhibitor for 3 weeks markedly reduced the proliferation of colonic adenoma cells, but resulted in little change in the proliferation rate or morphology of cells in the juxtaposed healthy intestinal mucosa (Waaler *et al.* 2012). These studies indicate that small molecule inhibitors of Axin degradation are promising agents for the targeted therapy of Wnt pathway-dependent diseases, and coupled with the work presented here, suggest that the conceptual framework needed to identify new therapeutic agents in this category relies on our ability to elucidate the distinct pathways that control endogenous Axin concentrations *in vivo*.

## Acknowledgments

We thank the investigators listed in *Materials and Methods* for generously sharing reagents and V. Marlar for technical assistance. We thank Claudio Pikielny, Ai Tian, and Hassina Benchabane for critical reading and thoughtful comments on this manuscript. This work was funded by grants from the National Institutes of Health (RO1CA105038 to Y.A., R01GM081635 and R01GM103926 to E.L., and P40OD018537 to the Bloomington *Drosophila* Stock Center), the Emerald Foundation (to Y.A.), the Norris Cotton Cancer Center (to Y.A.), and the National Science Foundation (DBI-1039423 for the purchase of a Nikon A1RSi confocal microscope).

## Literature Cited

Ahmed, Y., S. Hayashi, A. Levine, and E. Wieschaus, 1998 Regulation of armadillo by a Drosophila APC inhibits neuronal apoptosis during retinal development. Cell 93: 1171–1182.

Ahmed, Y., A. Nouri, and E. Wieschaus, 2002 Drosophila Apc1 and Apc2 regulate Wingless transduction throughout development. Development 129: 1751–1762.

Akong, K., E. E. Grevengoed, M. H. Price, B. M. McCartney, M. A. Hayden *et al.*, 2002 Drosophila APC2 and APC1 play overlapping roles in wingless signaling in the embryo and imaginal discs. Dev. Biol. 250: 91–100.

Baker, N. E., 1988 Transcription of the segment-polarity gene wingless in the imaginal discs of Drosophila, and the phenotype of a pupal-lethal wg mutation. Development 102: 489–497.

Bejsovec, A., and A. Martinez Arias, 1991 Roles of wingless in patterning the larval epidermis of Drosophila. Development 113: 471–485.

Bischof, J., R. K. Maeda, M. Hediger, F. Karch, and K. Basler, 2007 An optimized transgenesis system for Drosophila using germ-line-specific phiC31 integrases. Proc. Natl. Acad. Sci. USA 104: 3312–3317.

Brand, A. H., and N. Perrimon, 1993 Targeted gene expression as a means of altering cell fates and generating dominant phenotypes. Development 118: 401–415.

Brunner, E., O. Peter, L. Schweizer, and K. Basler, 1997 pangolin encodes a Lef-1 homologue that acts downstream of Armadillo to transduce the Wingless signal in Drosophila. Nature 385: 829–833.

Chen, B., M. E. Dodge, W. Tang, J. Lu, Z. Ma *et al.*, 2009 Small molecule-mediated disruption of Wnt-dependent signaling in tissue regeneration and cancer. Nat. Chem. Biol. 5: 100–107.

Chen, C. M., and G. Struhl, 1999 Wingless transduction by the Frizzled and Frizzled2 proteins of Drosophila. Development 126: 5441–5452.

Chou, T. B., and N. Perrimon, 1992 Use of a yeast site-specific recombinase to produce female germline chimeras in Drosophila. Genetics 131: 643–653.

Clevers, H., and R. Nusse, 2012 Wnt/beta-catenin signaling and disease. Cell 149: 1192–1205.

Couso, J. P., S. A. Bishop, and A. Martinez Arias, 1994 The wingless signalling pathway and the patterning of the wing margin in Drosophila. Development 120: 621–636.

Cselenyi, C. S., K. K. Jernigan, E. Tahinci, C. A. Thorne, L. A. Lee *et al.*, 2008 LRP6 transduces a canonical Wnt signal independently of Axin degradation by inhibiting GSK3′s phosphorylation of beta-catenin. Proc. Natl. Acad. Sci. USA 105: 8032–8037.

Fagotto, F., E. Jho, L. Zeng, T. Kurth, T. Joos *et al.*, 1999 Domains of axin involved in protein-protein interactions, Wnt pathway inhibition, and intracellular localization. J. Cell Biol. 145: 741–756.

Feng, Y., X. Li, L. Ray, H. Song, J. Qu *et al.*, 2014 The Drosophila tankyrase regulates Wg signaling depending on the concentration of Daxin. Cell. Signal. 26: 1717–1724.

Gerlach, J. P., B. L. Emmink, H. Nojima, O. Kranenburg, and M. M. Maurice, 2014 Wnt signalling induces accumulation of phosphorylated beta-catenin in two distinct cytosolic complexes. Open Biol. 4: 140120.

Golic, K. G., and S. Lindquist, 1989 The FLP recombinase of yeast catalyzes site-specific recombination in the Drosophila genome. Cell 59: 499–509.

Graham, F. L., and A. J. van der Eb, 1973 A new technique for the assay of infectivity of human adenovirus 5 DNA. Virology 52: 456–467.

Hamada, F., Y. Tomoyasu, Y. Takatsu, M. Nakamura, S. Nagai *et al.*, 1999 Negative regulation of Wingless signaling by D-axin, a Drosophila homolog of axin. Science 283: 1739–1742.

Huang, S. M., Y. M. Mishina, S. Liu, A. Cheung, F. Stegmeier *et al.*, 2009 Tankyrase inhibition stabilizes axin and antagonizes Wnt signalling. Nature 461: 614–620.

Kramps, T., O. Peter, E. Brunner, D. Nellen, B. Froesch *et al.*, 2002 Wnt/wingless signaling requires BCL9/legless-mediated recruitment of pygopus to the nuclear beta-catenin-TCF complex. Cell 109: 47–60.

Lau, T., E. Chan, M. Callow, J. Waaler, J. Boggs *et al.*, 2013 A novel tankyrase small-molecule inhibitor suppresses APC mutation-driven colorectal tumor growth. Cancer Res. 73: 3132–3144.

Lee, E., A. Salic, R. Kruger, R. Heinrich, and M. W. Kirschner, 2003 The roles of APC and Axin derived from experimental and theoretical analysis of the Wnt pathway. PLoS Biol. 1: E10.

Luo, W., A. Peterson, B. A. Garcia, G. Coombs, B. Kofahl *et al.*, 2007 Protein phosphatase 1 regulates assembly and function of the beta-catenin degradation complex. EMBO J. 26: 1511–1521.

MacDonald, B. T., K. Tamai, and X. He, 2009 Wnt/beta-catenin signaling: components, mechanisms, and diseases. Dev. Cell 17: 9–26.

Markstein, M., C. Pitsouli, C. Villalta, S. E. Celniker, and N. Perrimon, 2008 Exploiting position effects and the gypsy retrovirus insulator to engineer precisely expressed transgenes. Nat. Genet. 40: 476–483.

Nolo, R., L. A. Abbott, and H. J. Bellen, 2000 Senseless, a Zn finger transcription factor, is necessary and sufficient for sensory organ development in Drosophila. Cell 102: 349–362.

Parks, A. L., K. R. Cook, M. Belvin, N. A. Dompe, R. Fawcett *et al.*, 2004 Systematic generation of high-resolution deletion coverage of the Drosophila melanogaster genome. Nat. Genet. 36: 288–292.

Peterson-Nedry, W., N. Erdeniz, S. Kremer, J. Yu, S. Baig-Lewis *et al.*, 2008 Unexpectedly robust assembly of the Axin destruction complex regulates Wnt/Wg signaling in Drosophila as revealed by analysis in vivo. Dev. Biol. 320: 226–241.

Rogers, S. L., and G. C. Rogers, 2008 Culture of *Drosophila* S2 cells and their use for RNAi-mediated loss-of-function studies and immunofluorescence microscopy. Nat. Protoc. 3: 606–611.

Salic, A., E. Lee, L. Mayer, and M. W. Kirschner, 2000 Control of beta-catenin stability: reconstitution of the cytoplasmic steps of the wnt pathway in Xenopus egg extracts. Mol. Cell 5: 523–532.

Takacs, C. M., J. R. Baird, E. G. Hughes, S. S. Kent, H. Benchabane *et al.*, 2008 Dual positive and negative regulation of wingless signaling by adenomatous polyposis coli. Science 319: 333–336.

Tian, A., H. Benchabane, Z. Wang, and Y. Ahmed, 2016 Regulation of stem cell proliferation and cell fate specification by Wingless/Wnt signaling gradients enriched at adult intestinal compartment boundaries. PLoS Genet. 12: e1005822.

Tolwinski, N. S., M. Wehrli, A. Rives, N. Erdeniz, S. DiNardo *et al.*, 2003 Wg/Wnt signal can be transmitted through arrow/LRP5,6 and Axin independently of Zw3/Gsk3beta activity. Dev. Cell 4: 407–418.

Venken, K. J., J. W. Carlson, K. L. Schulze, H. Pan, Y. He *et al.*, 2009 Versatile P[acman] BAC libraries for transgenesis studies in *Drosophila melanogaster*. Nat. Methods 6: 431–434.

Vincent, J. P., C. H. Girdham, and P. H. O'Farrell, 1994 A cell-autonomous, ubiquitous marker for the analysis of Drosophila genetic mosaics. Dev. Biol. 164: 328–331.

Waaler, J., O. Machon, L. Tumova, H. Dinh, V. Korinek *et al.*, 2012 A novel tankyrase inhibitor decreases canonical Wnt signaling in colon carcinoma cells and reduces tumor growth in conditional APC mutant mice. Cancer Res. 72: 2822–2832.

Wang, Z., A. Tian, H. Benchabane, O. Tacchelly-Benites, E. Yang *et al.*, 2016 The ADP-ribose polymerase Tankyrase regulates adult intestinal stem cell proliferation during homeostasis in Drosophila. Development DOI: 10.1242/dev.127647.

Willert, K., C. Y. Logan, A. Arora, M. Fish, and R. Nusse, 1999 A Drosophila Axin homolog, Daxin, inhibits Wnt signaling. Development 126: 4165–4173.

Xu, T., and G. M. Rubin, 1993 Analysis of genetic mosaics in developing and adult Drosophila tissues. Development 117: 1223–1237.

Yang, E., O. Tacchelly-Benites, Z. Wang, M. P. Randall, A. Tian *et al.*, 2016 Wnt pathway activation by ADP-ribosylation. Nat. Commun. 7: 11430.

Zeng, L., F. Fagotto, T. Zhang, W. Hsu, T. J. Vasicek *et al.*, 1997 The mouse *Fused* locus encodes Axin, an inhibitor of the Wnt signaling pathway that regulates embryonic axis formation. Cell 90: 181–192.

Zhang, Y., S. Liu, C. Mickanin, Y. Feng, O. Charlat *et al.*, 2011 RNF146 is a poly(ADP-ribose)-directed E3 ligase that regulates axin degradation and Wnt signalling. Nat. Cell Biol. 13: 623–629.

*Communicating editor: M. F. Wolfner*

GENETICS

**Supporting Information**
www.genetics.org/lookup/suppl/doi:10.1534/genetics.115.183244/-/DC1

# Wnt/Wingless Pathway Activation Is Promoted by a Critical Threshold of Axin Maintained by the Tumor Suppressor APC and the ADP-Ribose Polymerase Tankyrase

**Zhenghan Wang, Ofelia Tacchelly-Benites, Eungi Yang, Curtis A. Thorne, Hisashi Nojima, Ethan Lee, and Yashi Ahmed**


DOI: 10.1534/genetics.115.183244

# Figure S1

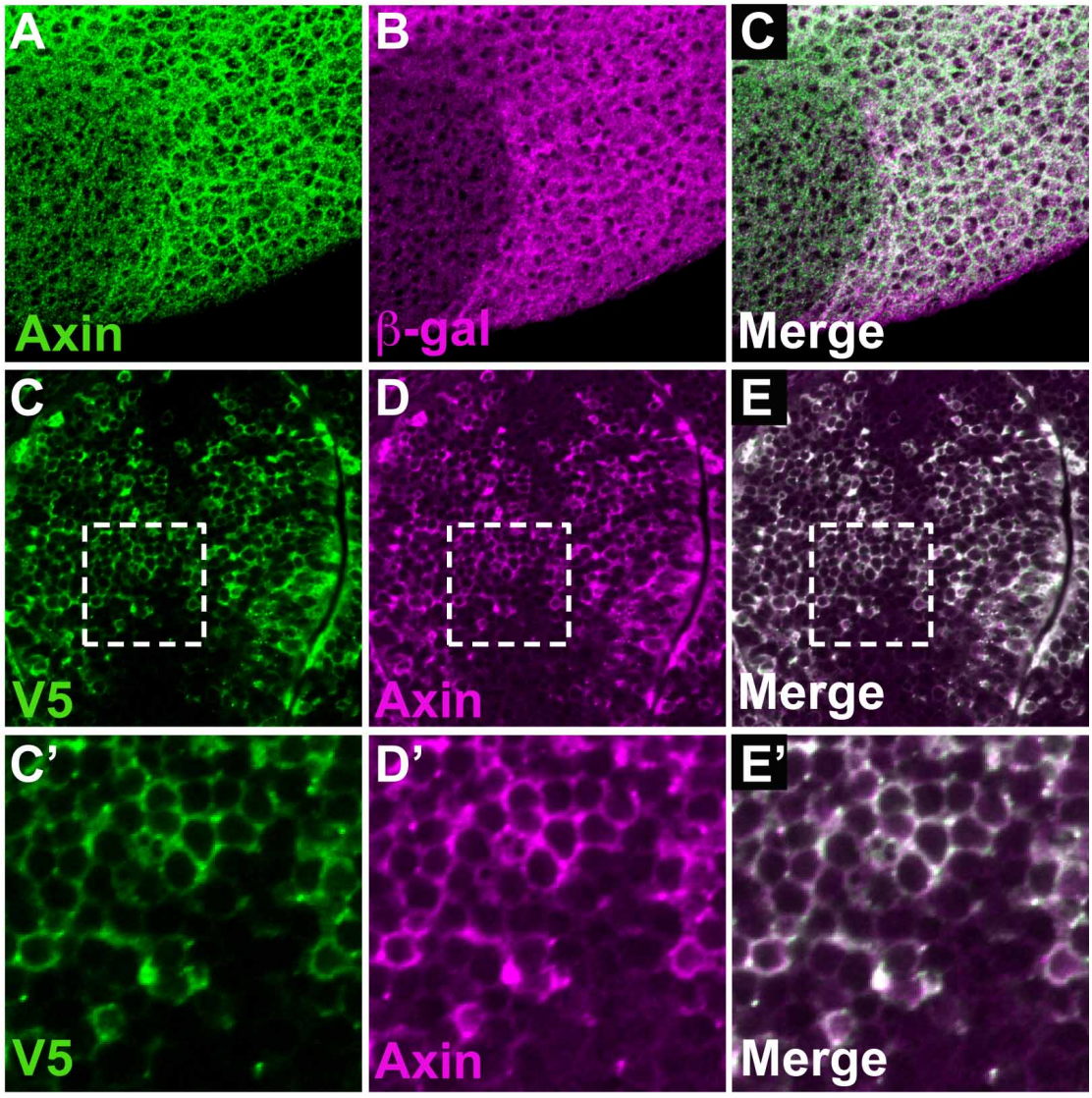


**Figure S1. Detection of Axin by immunostaining in imaginal discs**

(**A-C**) Confocal images of larval third instar wing disc labeled with α-Axin (green) and α-β-gal (magenta). *Axin*$^{18}$ null mutant clones (marked by the absence of β-gal, -/- in B) reveal the specificity of the Axin antibody. (**C-E**) Wing discs expressing Axin-V5 were labeled with α-V5 (green) and α-Axin (magenta). Higher magnification views of the boxed areas are shown in (**C'-E'**). Endogenous Axin levels are measured in the cells that are not labeled by V5 antibody.